Check for updates

Curcuphenols facilitate the immune driven attenuation of metastatic tumour growth

Samantha L. S. Ellis[1,2,3,4†], Lilian L. Nohara[1,2,3†], Sarah Dada[1,2,3,4,5,6], Iryna Saranchova[1,2,3,4,5,6], Lonna Munro[1,2,3,5], Kyung Bok Choi[1,2,3,5], Emmanuel Garrovillas[1,2,3,4,5,6], Cheryl G. Pfeifer[1,2,3,5], David E. Williams[7], Ping Cheng[7], Raymond J. Andersen[8] and Wilfred A. Jefferies[1,2,3,4,5,6]*

[1]Michael Smith Laboratories, University of British Columbia, Vancouver, BC, Canada, [2]Centre for Blood Research, University of British Columbia, Vancouver, BC, Canada, [3]The Djavad Mowafaghian Centre for Brain Health, University of British Columbia, Vancouver, BC, Canada, [4]Department of Microbiology and Immunology, University of British Columbia, Vancouver, BC, Canada, [5]Vancouver Prostate Centre, Vancouver Coastal Health Research Institute, Vancouver, BC, Canada, [6]Departments of Medical Genetics, Zoology, and Urologic Sciences, University of British Columbia, Vancouver, BC, Canada, [7]School of Medicine, Koç University, Istanbul, Türkiye, [8]Departments of Chemistry and Earth Ocean and Atmospheric Sciences, University of British Columbia, Vancouver, BC, Canada

One of the primary obstacles in current cancer treatments lies in the extensive heterogeneity of genetic and epigenetic changes that occur in each arising tumour. However, an additional challenge persists, as certain types of cancer display shared immune deficiencies in the antigen processing machinery (APM). This includes the downregulation of human leukocyte antigen (HLA) class I molecules, which serve as peptide antigen receptors for T lymphocyte recognition that plays a crucial role in killing emerging tumours. Consequently, this contributes to immune escape in metastatic disease. Notably, current cell-based immunotherapies primarily focusing on T lymphocytes and the implementation of immune checkpoint inhibitor modalities have largely ignored the crucial task of reversing immune escape. This oversight may explain the limited success of these approaches becoming more effective cancer immunotherapies. Hence, there is a critical need to prioritize the discovery of new therapeutic candidates that can effectively address immune escape and synergize with evolving immunotherapy strategies. In this context, we identified curcuphenol in a cell-based screen from a library of marine extracts as a chemical entity that reverses the immune-escape phenotype of metastatic cancers. To advance these findings toward clinical efficacy, the present study describes the synthesis of analogues of naturally occurring curcuphenol with enhanced chemical properties and biological efficacy. Here we test the hypothesis that these curcuphenol analogues can evoke the power of the immune system to reduce the growth of metastatic disease in tumour bearing animals. Our findings indicate that these compounds effectively restore the expression of APM genes in metastatic tumours and inhibit the growth of highly invasive tumours in preclinical models, thereby counteracting the common immune evasion phenomenon observed in metastatic cancers. We conclude that cancer

immunotherapies capable of boosting APM expression, hold great potential in maximizing the effectiveness of immune blockade inhibitors and eradicating invasive tumours.

Introduction

Metastatic cancer is responsible for approximately 90% of cancer-related deaths (McGranahan and Swanton, 2017) which highlights the urgent necessity to understand the mechanisms driving the transition from primary to metastatic sequalae. The human leukocyte antigen (HLA) system, also known as the major histocompatibility complex (MHC) in humans, constitutes a pivotal component of the adaptive immune response to emerging cancers. These molecules act as peptide receptors to present antigenic peptides to the T-cell receptor (TCR) found on T lymphocytes, which are integral cellular components of the adaptive immune system. This sophisticated mechanism not only restricts the development of tumours but also facilitates the elimination of infected cells, underlying its crucial role in immunity (Alimonti et al., 2000). During the evolution of metastasis, transition results from the accumulation of genetic and epigenetic changes often facilitated by the selective pressure of the host immune system. This process termed immune escape or immune editing results in the emergence of variants that are subsequently invisible to immune surveillance, thereafter allowing cancer cells to proliferate unchecked by the host immune system that selected them (Alimonti et al., 2000; Shankaran et al., 2001). These evasion mechanisms include tumour-induced T-cell anergy, diminished or absent major histocompatibility complex -1 (MHC-1) MHC-I expression, defects in the MHC-I antigen processing machinery (APM), and disruptions of the newly activated IL-33/MHC-I autocrine mechanism (Jefferies et al., 1993; Gabathuler et al., 1994; Marusina et al., 1997; Gabathuler et al., 1998; Alimonti et al., 2000; Shankaran et al., 2001; Zhang et al., 2002; Vitalis et al., 2005; Lou et al., 2007; Zhang et al., 2007; Lou et al., 2008; Setiadi et al., 2008; Newman and Cragg, 2016a; Saranchova et al., 2016; Saranchova et al., 2018; Dada et al., 2023). Moreover, a clear association has been established between downregulation of MHC-I and poor prognosis across various cancer types, including lung (Blades et al., 1995; Naoe et al., 2002; Zhang et al., 2003), breast (Alpan et al., 1996; McDermott et al., 2002), renal (Kitamura et al., 1997), melanoma (Kamarashev et al., 2001; Chang et al., 2006), colorectal (Cabrera et al., 2005), head and neck squamous cell (Andratschke et al., 2003), cervical (Mehta et al., 2008) and prostate cancers (Saranchova et al., 2016). Given that only 15–30% of patients respond to current immunotherapies, the need to discover new and enhanced treatment options, along with advanced methods for patient selection, becomes a pressing societal concern. Overcoming the immune evasion mechanisms that underlie tumour resistance to existing immune therapies is essential to achieving the full potential of cancer immunotherapy for solid tumours. Several small molecules capable of reversing the loss of expression of MHC-I in metastatic tumours have been described, such as histone deacetylase inhibitors (HDACi) (Setiadi et al., 2005; Setiadi et al., 2007a; Setiadi et al., 2008), and cannabinoids (Dada et al., 2022), thus the potential of small

molecules to counter immune evasion remains highly promising as mainstream drugs for countering metastatic disease.

Historically, natural products have served as a rich source for the development of anti-cancer drugs, with nearly half of all new anti-cancer drugs in the past century, including paclitaxel, vincristine, doxorubicin, and bleomycin (Cragg et al., 2012; Huang et al., 2021), originating from natural extracts (Newman and Cragg, 2016). Dietary items like spices and herbs have long been associated with medicinal properties, although the progression from recognizing their broad biological impacts, often referred to as nutraceutical or bioceutical effects, to attributing specific therapeutic benefits to distinct bio-active molecules remains elusive.

Turmeric and cumin, studied by ethnobotanists for their culinary, dietary, and medicinal uses, offer potential remedies for various ailments, including arthritis, digestive and respiratory disorders, allergies, liver disease, depression, and cancer (Soflaei et al., 2018). The beneficial properties of these natural products are primarily attributed to curcuminoids. However, their therapeutic application has been constrained due to challenges such as low water solubility, chemical instability, vulnerability to acidic conditions, poor absorption, and rapid breakdown (Soflaei et al., 2018). Moreover, identifying the specific molecular entities responsible for distinct medicinal benefits necessitates further investigation.
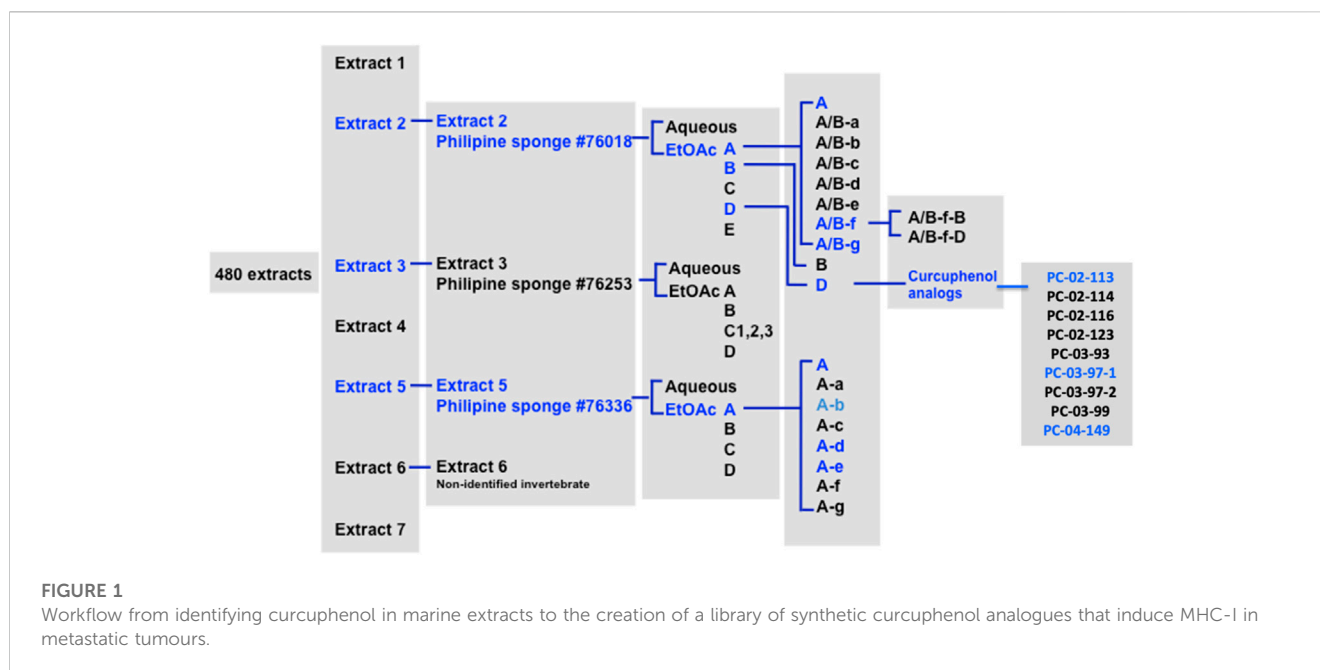
Recently, we focused on the anti-cancer effects of curcuphenol, a curcuminoid naturally occurring in spices such as turmeric and cumin, as well as in marine invertebrates. Initiated, through the screening of a library of natural marine extracts, curcuphenol was identified as a compound capable of reversing MHC-loss *in vitro* (Nohara et al., 2023). Subsequently, we demonstrated that curcuphenol possesses an unusual HDAC-enhancing activity that promotes the expression of APM genes in invasive metastatic tumours (Ellis et al., 2023).

Here we have chemically synthesized several unique curcuphenol analogues with enhanced chemical characteristics and explored their potential to reduce the growth of metastatic tumours in preclinical animal models. We test the hypothesis that these curcuphenol analogues induce APM expression and reduce the growth of metastatic disease in tumour bearing animals.

Results

Curcuphenol induces the expression of the APM components, MHC-I, TAP1 and LMP molecules, in metastatic tumour cells

As described previously (Nohara et al., 2023), initially a library of 480 marine invertebrate extracts was screened. TAP-1 is an important molecule involved in antigen processing and presentation. The purpose of this high-throughput cell-based screening assay was to

FIGURE 1
Workflow from identifying curcuphenol in marine extracts to the creation of a library of synthetic curcuphenol analogues that induce MHC-I in metastatic tumours.

assess the increase in TAP-1 promoter-induced green fluorescent protein (GFP) expression in the APM-deficient LMD pTAP-1 metastatic prostate cancer cells. To evaluate the activity of each marine extract, the percentage of TAP-1 induction was calculated by standardizing the GFP fluorescence intensity of each extract to the average fluorescence intensity of the 1% dimethylsulfoxide (DMSO) vehicle control. Additionally, the fluorescence intensity of each extract was compared to the GFP fluorescence intensity of the positive control, which was stimulated with interferon γ (IFNγ), a known inducer of TAP-1 expression. Based on the screening results, marine extracts were selected for further investigation and subsequently fractionated to identify curcuphenol as the active chemical entity capable of reversing MHC-loss *in vitro* (Figure 1). The active component identified as S- (+)-curcuphenol via NMR and optical rotation, was isolated from sponge extracts as previously described (Nohara et al., 2023) and in the workflow in Figure 1.

In this study we extend our studies to tumours from other tissues beyond prostate cancers. The TC-1 cell line, derived from primary lung epithelial cells of a C57BL/6 mouse, was immortalized using the LXSN16 retrovirus vector carrying Human Papillomavirus E6/E7 oncogenes. Additionally, TC-1 cells were transformed with a pVEJB plasmid expressing the activated human H-Ras oncogene, endowing them with oncogenic properties and tumorigenic potential. The A9 cell line, representing the metastatic variant of TC-1 cells, resulted from in vivo immunization procedures in animals bearing the original TC-1 parental cells. This immunization favored the selection of clones with enhanced immune resistance, leading to the establishment of the A9 cell line, characterized by immune escape or immune editing. Notably, a key distinction between TC-1 and A9 cells lies in their MHC-I expression levels, with TC-1 cells displaying high expression while A9 cells exhibit nearly undetectable levels (Smahel et al., 2003).

Our results demonstrate that curcuphenol augments the expression of surface MHC-I protein in lung metastatic A9 cells (Figure 2A). We ascertained that a concentration of 76.7 uM was

optimum for enhancing MHC-I expression while maintaining cell viability (Figure 2A). Notably, curcuphenol-induced A9 cells exhibited similar surface MHC-I protein expression compared to primary TC-1 cells (Figure 2B). IFNγ, used as a positive control, induced a significant increase in MHC-I protein expression in metastatic A9 cells. Compared to the vehicle control of 1% DMSO, stimulation with curcuphenol resulted in increased mRNA expression of the APM molecules MHC-I, TAP1, and LMP, with an RQ of 24.2 ($p < 0.05$), ($p < 0.001$), and 2.77 ($p < 0.01$), respectively (Figure 2C).

Screening and synthesis of curcuphenol analogues with MHC-I inducing activity

Subsequently, we synthesized a library of synthetic analogues (Figure 3A and 3B) as described in the materials and methods and tested for their ability to induce MHC-I in metastatic A9 cells (Figures 3C,D). From these studies, the curcuphenol analogues PC-02-113 (McDermott et al., 2002) and PC-03-97-1 (Zhang et al., 2003) were confirmed to be the most active in the induction of MHC-I expression in metastatic A9 cells (Figures 3C,D).

Measurement of antigen presentation by curcuphenol-treated metastatic lung tumours

We employed CD8^{+} T lymphocytes derived from homozygous transgenic mice expressing the mouse Tcrα-V2 and Tcrβ-V5 genes to assess the induction of antigen processing and presentation in metastatic A9 tumours by curcuphenols. The engineered T cell receptor present in these mice has been specifically tailored to identify a sequence of amino acids (residues 257–264) found
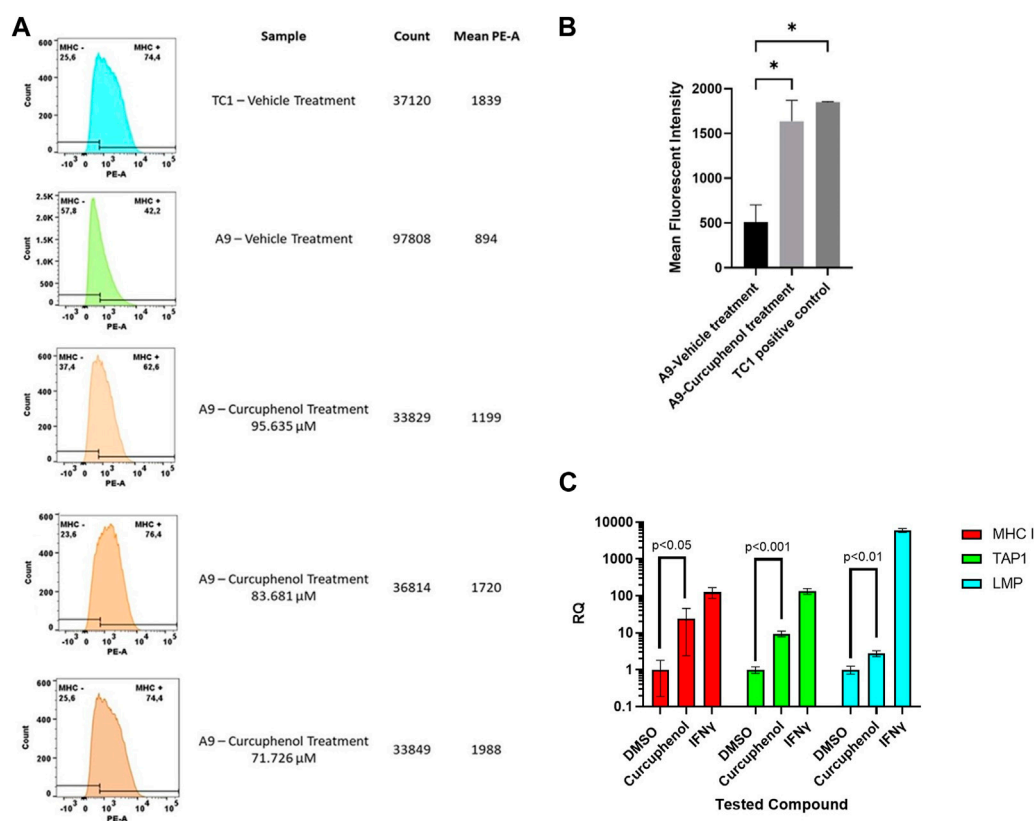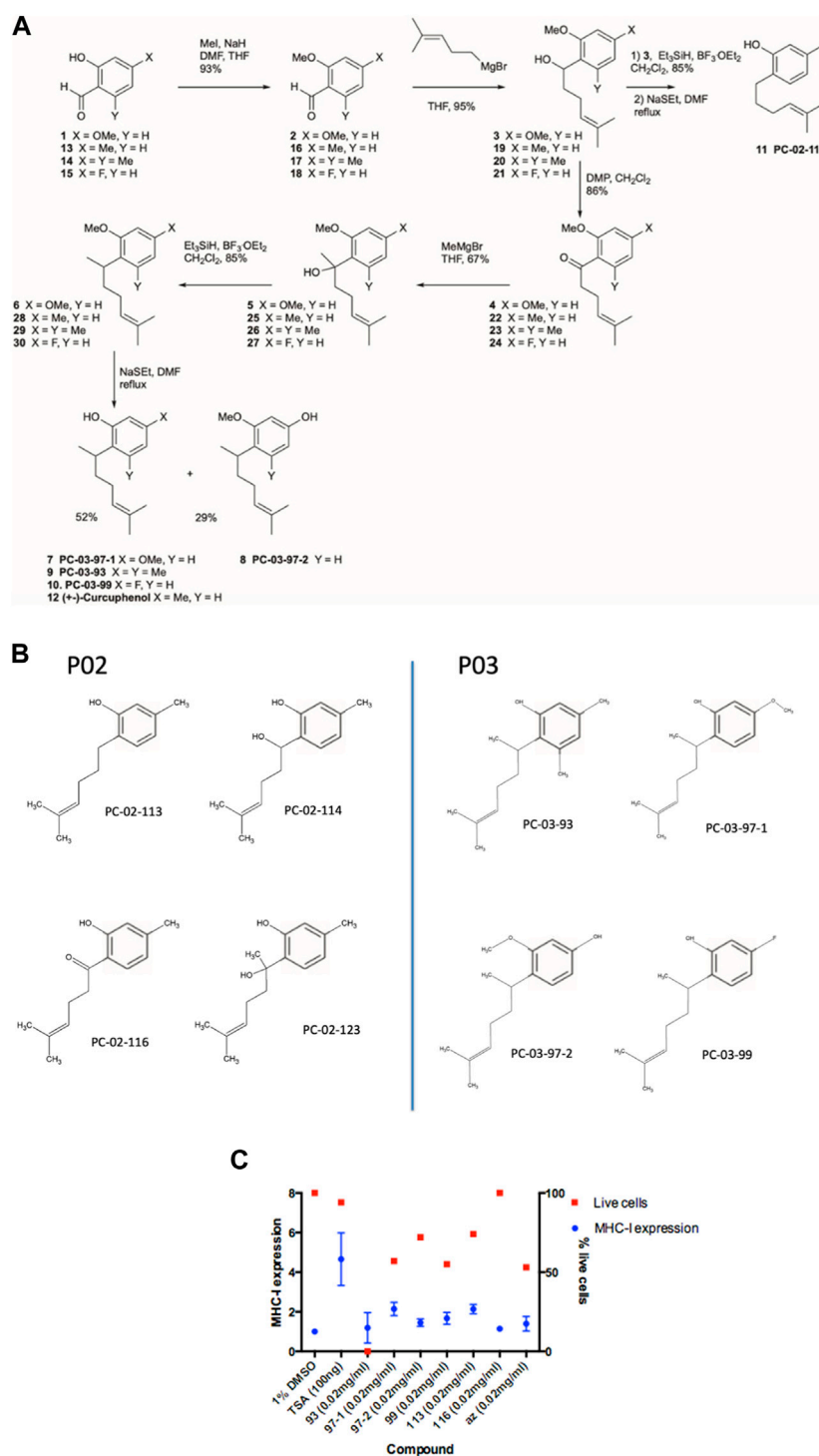
FIGURE 2
Confirmation that curcuphenol treatment enhances surface MHC- I expression **(A)** Metastatic A9 lung tumour cells were treated with either vehicle (DMSO) or curcuphenol for 48 h. Primary TC-1 tumours cells that constitutively express MHC-I were used as a positive control. The cells were then harvested and subjected to flow cytometry. The experiment was repeated three times. **(B)** The statistical test was done using ANOVA. The mean fluorescent intensity of metastatic A9 tumour cells untreated and the DMSO treatment was pooled as control population. The values of three curcuphenol treatments of metastatic A9 tumour cells were pooled together for the treated group. A two-tailed t-test was conducted with a cut-off of p-value of 0.05 and below considered significant. The paired t-test resulted in a p-value of 0.01 which being less than 0.05 is considered significant. This experiment was repeated 3 times **(C)** Curcuphenol increased mRNA expression of MHC-I, TAP1, and LMP, in A9 cells. RNA was isolated and reverse transcribed into cDNA for Real-Time PCR analysis. Samples were run in triplicate (n = 3) on a 7,500 Fast Real-Time PCR system (Applied Biosystems). Relative Quantification (RQ) was calculated by the 7,500 Fast Real-Time PCR system software. Values were normalized to Housekeeping gene SDHA106 and calculated with 1% DMSO treatment as reference. Data was visualized and subjected to an ANOVA statistical analysis using GraphPad Prism 9.

within ovalbumin (Hogquist et al., 1994). This recognition occurs in conjunction with the H2K^b molecule, a murine MHC-I molecule (Falk et al., 1991). These mice serve as a valuable model for investigating the involvement of peptides in the processes of positive selection within the immune system's T lymphocytes. Furthermore, they provide insights into how CD8$^+$ T lymphocytes, a subset of immune cells, react to antigens presented by this transgenic T cell receptor (Carbone et al., 1992).

To evaluate the induction of antigen presentation by curcuphenol-treated metastatic A9 tumours in an OT1 CFSE proliferation assay involved using CD8$^+$ T lymphocytes from SIINFEKL-specific OT1 mice, we assessed the response to the SIINFEKL peptide presented on MHC- I of A9 metastatic cells (Figure 4). The A9 cells were treated with curcuphenol or IFNγ (positive control). Carboxyfluorescein diacetate succinimidyl ester (CFSE)-labeled OT1 T lymphocytes alone were used as a negative control. A9 cells present the SIINFEKL peptide on MHC-I molecules. CD8$^+$ T lymphocytes from SIINFEKL-specific

OT1 mice were used. These T lymphocytes recognize the SIINFEKL peptide-MHC complex. CFSE dye labels cells and allows tracking of cell divisions. As cells divide, the dye gets diluted, leading to decreased fluorescence in daughter cells. At generation 1 there was no significant difference in proliferation between curcuphenol-treated cells and the uninduced vehicle-treated group. Starting from generation 2, the curcuphenol-treated group showed significantly higher proliferation compared to both the uninduced vehicle-treated group and the CFSE-labeled OT1 T lymphocytes alone (negative control). The results show that while there was no difference in the initial round of cell divisions (generation 1), curcuphenol-treated cells showed increased T lymphocyte proliferation ($p < 0.0001$) in subsequent generations (generation 2 onward) compared to untreated A9 cells or T lymphocytes alone (Figure 4). This indicates that curcuphenol treatment enhances the antigen presentation process, leading to more effective activation and proliferation of CD8$^+$ T lymphocytes.

FIGURE 3
Synthesis and assessment of synthetic curcuphenol analogues that induce MHC-I in metastatic tumours cells. **(A)** The process for the synthesis of curcuphenol analogues. **(B)** Chemical structure of synthetic curcuphenols. **(C)** Benchmarking series PC-02 synthetic curcuphenols analogues against TSA in MHC-I induction. PC-02-113 and PC-03-97-1 curcuphenol analogs induce MHC-I expression. The blue bars refer to the expression of the protein complex, MHC-I, on the cell surface, as assessed by flow cytometry. The percentage of live cells in the sample as a read-out of drug toxicity, as assessed using propidium iodide staining (in red). The experiments were replicated twice (n = 2) to ensure precision in determining the mean fluorescence of MHC-I expression. Compounds exhibiting over 40% activity compared to TSA and demonstrating minimal cytotoxic effects (cell viability within one standard deviation of the negative control represented) were identified as potential candidates for subsequent analysis. Antigen presentation is increased by curcuphenol-treated metastatic lung carcinomas.
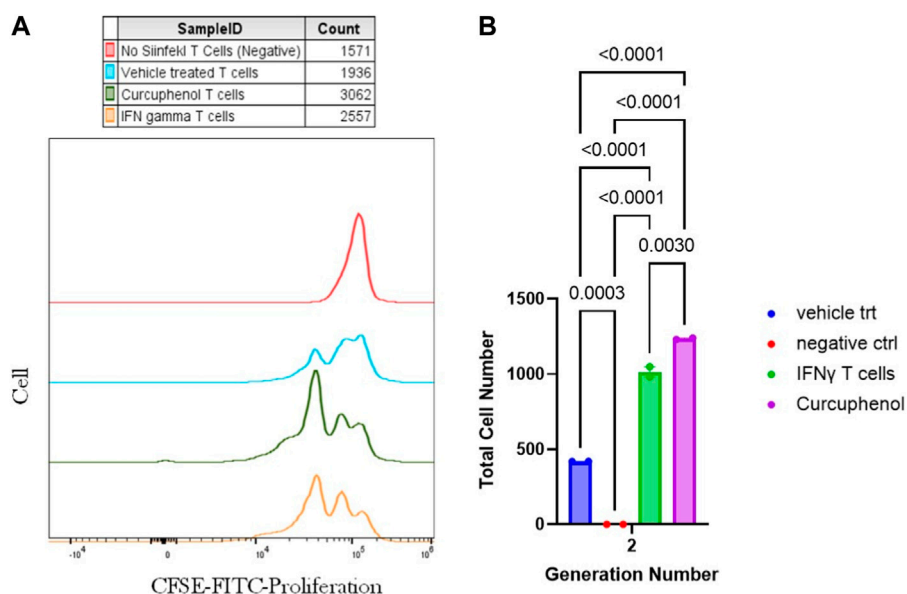
FIGURE 4
Measurement of antigen presentation by curcuphenol-treated metastatic lung tumours. **(A)** The evaluation of antigen presentation by curcuphenol-treated metastatic A9 tumours in an OT-I CFSE proliferation assay involved using CD8^{+} T cells from SIINFEKL-specific OT1 mice to respond to the SIINFEKL peptide presented on MHC class I of A9 cells. A9 cells were treated with 0.00167 μmol/mL of curcuphenol or 5.832 × 10^{−6} nmol/mL of IFNγ as a positive control. The negative control consisted of OT1 cells alone labeled with CFSE proliferation dye, which decreases within the daughter cells as the generations progress. **(B)** At generation 1, there was no significant difference in proliferation between the curcuphenol PO3 analog-treated cells and the uninduced vehicle (peptide) treated group. However, from generation 2 onward, the curcuphenol-treated group exhibited significantly higher proliferation compared to the uninduced vehicle (peptide) treated group or the CFSE-labeled OT1 T cells alone. Each p-values are shown above the comparisons.
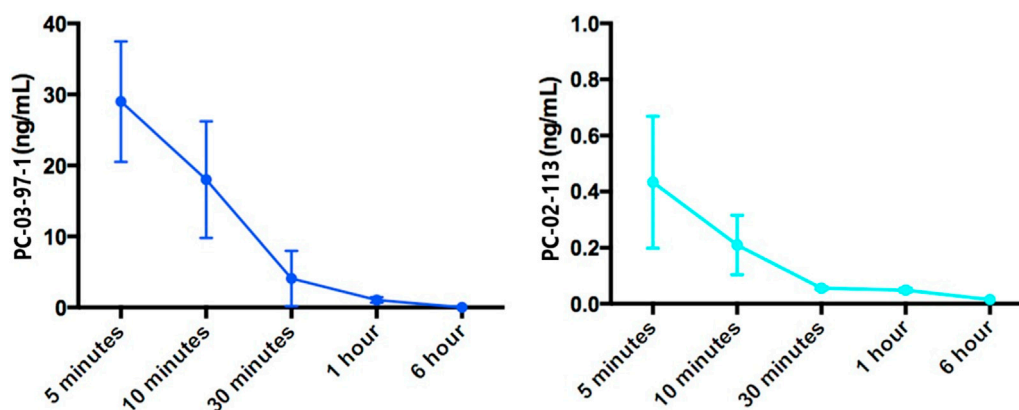

FIGURE 5
Pharmacokinetic analysis of PC-02-113 and PC-03-97-1: The average concentration of PC-02-113 and PC-03-97-1 in mouse plasma from three mice at each time point is shown with SEM. Female C57BL/6 mice, aged 6−8 weeks, received an i. p. injection of 5.2 mg/kg of PC-02-113 or PC-03-97-1, and blood was collected through cardiac puncture at different time points (n = 3) after injection. Plasma was separated from blood and sent to the Metabolomics Innovation Center (TMIC) at the UVIC Genome BC Proteomics Centre for pharmacokinetic analysis. All tests were conducted utilizing a UPLC-4000 QTRAP system equipped with Electrospray Ionization (ESI) and positive ion detection. A C18 column was employed, and the mobile phase consisted of acetonitrile, water, and formic acid.

Pharmacokinetics of PC-02-113 and PC-03-97-1 to one in tumour-bearing mouse model

Next, the pharmacokinetics of PC-02-113 and PC-03-97-1 were studied following intraperitoneal injection into rats at different time points, to inform a suitable *in vivo* dosing regimen. We elected time points based on the reported metabolism of Trichostatin A (TSA), a compound with structural similarities to curcuphenol and cannabinoids, other chemical entities that reverse immune escape (Smahel et al., 2003;
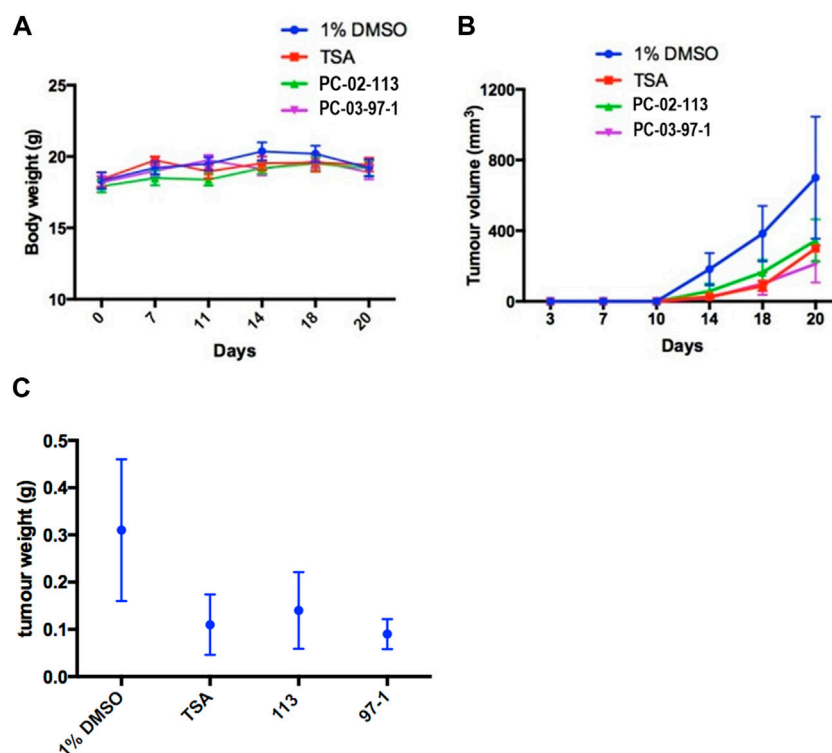
FIGURE 6

In vivo treatment with PC-02-113 or PC-03-97-1 hinders the growth of APM–deficient metastatic A9 lung cancer cells. A9 cells were injected subcutaneously into the right flank. After 7 days, mice were divided into four treatment groups: (a) 1% DMSO vehicle negative control, (b) TSA (0.5 mg/kg), (c) PC-02-113 (5.2 mg/kg), and (d) PC-03-97-1 (5.2 mg/kg). After 12 days of treatment, tumours were excised and analyzed for CD4$^+$ and CD8$^+$ T lymphocyte infiltration using flow cytometry. **(A)** Body weights remained unaffected by the compounds, suggesting no toxicity. **(B)** TSA, PC-02-113, and PC-03-97-1 significantly reduced tumour growth in comparison to the DMSO control established by a one-tailed *t*-test ($p < 0.0001$). **(C)** A9 metastatic lung tumour weight was reduced with P02-113 and P03-97-1 treatment compared to vehicle. TSA, PC-02-113, and PC-03-97-1 reduces mean tumour weight in comparison to the DMSO controls.

Dada et al., 2022). Despite their similarities, the analogues exhibited significantly different profiles. For instance, PC-03-97-1 presented a half-life of 15 min, while PC-02-113 demonstrated a half-life of less than 5 min. Both compounds were undetectable in mouse plasma at the 6-h mark. Given these pharmacokinetic profiles and constraints of dosing regimens, we opted for daily treatment in our *in vivo* studies (Figure 5).

Curcuphenol analogues attenuates the growth of metastatic tumours

Following the subcutaneous injection of 4×10^5 A9 metastatic mouse lung cancer cells into the right flank, tumours were allowed to develop for 7 days (Figure 6A). Subsequently, the mice underwent daily treatments for 12 days with TSA, 1% DMSO, or the experimental compounds, PC-02-113 or PC-03-97-1. Across all groups, body weight did not show significant variances demonstrating the compounds are well tolerated (Figure 6A). A significant reduction in tumour volume and size was observed in groups treated with the curcuphenol analogues PC-02-113 and PC-03-97-1 compared to the untreated group (1% DMSO) ($p < 0.0001$) (Figures 6B,C).

Curcuphenol analogues augment tumour-infiltrating lymphocytes

Both compounds, PC-02-113 and PC-03-97-1, exhibited promising anti-cancer properties *in vitro* and *in vivo*. Their potential to induce TAP-1 and MHC-I expression positions them as promising candidates for clinical trials, especially in light of the downregulation of these proteins observed in specific cancer types. Endpoint T-lymphocytes infiltration of tumours was also assessed to understand the anti-tumour mechanisms of these compounds. Tumour infiltrating lymphocytes (TILs) were evaluated using flow cytometry to CD4$^+$ and CD8$^+$ T lymphocytes subpopulations (Figure 7). CD8$^+$ T-lymphocyte infiltration reflected the pattern of tumour burden. Among the groups, TSA and PC-03-97-1 showed the highest CD8$^+$ T lymphocytes penetration. No substantial variations in CD4$^+$ T lymphocytes infiltration were found across the groups. These findings suggest that PC-03-97-1 acts as a potent *in vivo* immunostimulant, exhibiting a significant reduction in tumour burden. Consequently, future investigations should focus on the optimization of PC-03-97-1's structure (Figure 7).
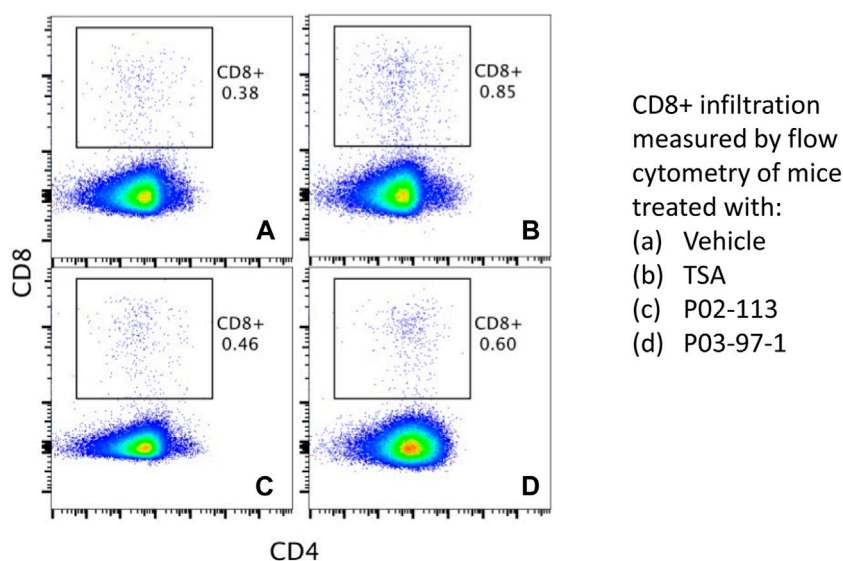
FIGURE 7
Evaluation of T cell infiltration in metastatic tumours *in vivo*. P02-113 and P03-97-1 treatment group has increased CD8$^+$ T cell infiltration into tumour-boosts immunity. C57BL/6 mice were injected subcutaneously in the right flank with 5×10^4 APM-deficient metastatic A9 lung cancer cells. Seven days post-injection, mice were assigned to four treatment groups: vehicle **(A)**, TSA (0.5 mg/kg) **(B)**, PC-02-113 (5.2 mg/kg) **(C)**, or PC-03-97-1 (5.2 mg/kg) **(D)**. After 12 days of treatment, tumours were excised and assessed for CD4$^+$ (APC) and CD8$^+$ (PE-Cy7) TIL infiltration using flow cytometry. The numbers inset refer to the percentage of CD8$^+$ or CD4$^+$ cells within the tumour mass assessed by Flow cytometry.

Discussion

This study aimed to explore the potential of specific curcuminoids, to leverage the immune system's power to combat and ultimately eradicate metastatic cancers by countering immune evasion. Curcuphenol, a constituent found in culinary spices like cumin and turmeric, has a long history of traditional use in medicinal ethnobiology and ethnopharmacology as both dietary supplements and traditional remedies (Dada et al., 2022). Previous studies demonstrated the potential of curcuminoids, such as curcuphenols, to reverse immune evasion in metastatic tumours *in vitro* (Ellis et al., 2023; Nohara et al., 2023) but no previous study assessed the ability of curcuphenols to reduce the growth of tumours in animals. To understand the underlying mechanism behind this phenomenon, we investigated the impact of curcuphenols on histone deacetylases activity (HDAC) activity. Our findings revealed that curcuphenols possess a unique HDAC-enhancing activity, leading to alterations in epigenetic marks, particularly H3K27ac, which subsequently induce the expression of APM components in metastatic prostate and lung cancer cells. Interestingly, our analysis using H3K27ac Chromatin Immunoprecipitation Sequencing (ChIP-seq) demonstrated that the induced epigenomic changes closely resemble the genome-wide patterns observed with IFNγ, a well-known master regulator of both innate and adaptive immune responses, including those against tumours. This highlights the potential implications of dietary components and their analogues in modulating immune responses.

Despite efforts to enhance bioavailability through innovative formulations, such as edible microparticles or nanoparticles (Zheng and McClements, 2020), the chemical diversity of curcuminoids and the lack of standardization across various studies present considerable challenges. To translate the use of

curcuminoids into clinical practice for diseases like cancer, it is crucial to identify individual curcuminoid molecules and elucidate their specific mechanisms of action. To address these limitations, we have synthesized analogues of curcuphenol, exhibit improved chemical properties and biological efficacy (described Figures 2, 4).

Curcuphenol occurs naturally as one of two enantiomers: S- (+) and R- (−) curcuphenol (Fusetani et al., 1987; Wright et al., 1987; El Sayed et al., 2002; Gaspar et al., 2004; Cichewicz et al., 2005; Gaspar et al., 2008; Rodrigo et al., 2010; Behery et al., 2012), however in many applications only the S- (+) of curcuphenol is biologically active (Figure 2). Therefore, a pharmacopoeia of analogues of curcuphenol were synthesized in this study with the aim of finding more effective, achiral analogues. Furthermore, curcuminoids are generally insoluble in water and we used simple chemical synthesis methods to create water soluble, and achiral curcuphenol analogue PC-02-113 and a racemic analogue PC-03097-1 that are soluble in both phosphate buffer saline and water, that also have enhanced chemical characteristics and biological performance. We subsequently demonstrated their ability to enhance the expression of APM components which results in the reversal of the immune-escape phenotype in metastatic tumours both *in vitro* (Figure 5) and *in vivo* (Figure 6). Clearly, these new curcuphenol compounds have advantages in solubility and ease of synthesis and can be used as singular molecular entities rather than plant or animal extracts that contain many, sometimes counteractive chemical entities. We subsequently demonstrated their ability to inhibit the growth of invasive, metastatic tumours by enhancing the expression of APM components. The two enhanced curcuphenol-based analogues, PC-02-113 and PC03- 97- 1, that we previously demonstrate have histone deacetylase inhibitors (HDACi) enhancing activities (Ellis

et al., 2023), are well-tolerated *in vivo*, with no observable toxicity in animals at the examined dosages. Administrating these compounds to mice bearing established metastatic tumours led to a statistically significant decrease in average tumour size. Overall, PC-03-97-1 demonstrates a more potent effect *in vivo*, making it a promising candidate for undertaking future clinical trials. However, optimization of the dosage of PC-03-97-1 and further chemical modification of the scaffold to increase its plasma half-life may be necessary as it has been shown to have a high clearance rate from the plasma of rats (Figure 4). This may be overcome by delivery in formulations such as lipid nanoparticles or in other slow release formulations.

Studies conducted *in vitro* indicate that curcuphenol reverses the MHC-I immune-escape of metastatic tumours and thereby revealing the tumour to immune recognition and enhancing effector CD8^{+} T lymphocytes detection of metastatic tumours (Figure 2). In our studies, no increase in the frequency of CD4^{+} tumour infiltrating T lymphocytes was observed though it is conceivable that the activation and functional status of these cells may have changed in curcuphenol-analogue treated animals. However, a 2-fold increase in frequency of CD8^{+} tumour infiltrating T lymphocytes was observed (Figure 7). Despite this, it is difficult to determine from the literature the functional significance of a 2-fold increase in CD8^{+} tumour infiltrating T lymphocytes amongst the tumour mass. It could suggest either the metastatic tumour growth inhibiting effect we observe could be due to this increase in CD8^{+} tumour infiltrating T lymphocytes or perhaps due to a systemic increase in recirculating tumour specific T lymphocytes. Alternatively the effect we observe is due to the added contribution of other leukocyte population we are not measuring, such as natural killer cells and dendritic cells, or that the growth inhibiting effect is due to another mechanism that requires discovery. Future lines of investigation will be needed to resolve this question.

The significance of targeting the reversal of immune escape in oncology can perhaps be best understood by examining the historical context of the ignorance of this mechanism significantly curtailed the emergence of the entire field of cancer immunotherapies. In 1974, Stutman's presented evidence showing no significant difference in tumour growth between athymic nude mice (lacking T-lymphocytes) and wild-type mice and concluded that the adaptive cellular immune response does not play a role in cancer immune surveillance (Stutman, 1974; Fridman, 2018). However, a key crucial oversight in these studies was the use of tumours subsequently shown to lack APM capabilities. As a result, the tumours were effectively "invisible" to the host adaptive immune system, rendering the presence or absence of T-lymphocytes irrelevant to immune surveillance mechanisms because immune escape had already occurred in the tumours which Stutman was studying. After many years, these findings were finally directly refuted by Alimonti et al., in 2000 (Alimonti et al., 2000), who revisited Stutman's experiments from a new perspective. Alimonti et al. (2000) explored the growth of tumours with intact APM (immune competent) and tumours lacking APM (immune escape) in both athymic nude mice and wild-type mice. This investigation provided compelling evidence that T-lymphocytes and therefore the adaptive cellular immune response is indeed necessary for cancer immune surveillance, but their effectiveness depends on the coincident expression of functional APM and MHC-I in the

tumour. This study laid the foundation for understanding the complex dynamics of immune interactions with tumours and opened avenues for subsequently leveraging the profound power of T lymphocytes in cancer immunotherapy.

As a result of this early work, APM deficiencies are now widely recognized as immune escape and is associated with metastatic cancers (Alimonti et al., 2000; Saranchova et al., 2016) and have shown a clear correlation between downregulation of HLA and poor prognosis (Alpan et al., 1996; Kitamura et al., 1997; Kamarashev et al., 2001; McDermott et al., 2002; Andratschke et al., 2003; Cabrera et al., 2005; Chang et al., 2006; Mehta et al., 2008). In some tumour types, up to 90% of patients exhibit the loss of APM components and functional HLA molecules, indicating immune escape. This phenomenon is often associated with increased tumour invasiveness and higher metastatic potential (Blades et al., 1995; Naoe et al., 2002; Zhang et al., 2003) but may be the common Achilles-heel of most aggressive cancers. However, it follows that most immunotherapies targeting metastatic cancers must simultaneously address immune escape mechanisms while also enhancing anti-cancer cell-mediated immune responses. Unfortunately, most emerging cell-based immuno-therapeutics utilizing T lymphocytes and immune checkpoint blockage inhibitors profoundly ignored the need to reverse immune escape and this may explain why they often fail in clinical trials of cancer immunotherapies. Currently, only 15%–30% of patients respond to existing immunotherapies (Seliger, 2016; Dhatchinamoorthy et al., 2021), and hence, discovering new therapeutic candidates that overcome immune-escape and augment the evolving immunotherapy modalities should be a priority. Therefore, combination therapies where the addition of small molecule drugs such as curcuphenols that resurrect APM expression, may be the key to unlocking the true power of the immune system to eradicate invasive cancers (Lankat-Buttgereit and Tampé, 2002; Setiadi et al., 2005; Setiadi et al., 2007b; Setiadi et al., 2008).

The study provides encouraging results in preclinical models and undoubtedly provide a foundation for potential clinical applications. It addresses many of the limitations in actuating curcuminoids into clinical practice by creating simple methods to create new bioactive synthetic analogues of curcuphenol that have greater solubility than their natural counterpart and some of the analogues do not have a chiral bond rendering the synthesis more scalable. However, the translation from promising preclinical findings to practical clinical applications is often intricate and fraught with challenges. One significant hurdle lies in the complex realm of bioavailability when it comes to curcuminoids, the active compounds being studied. Factors such as metabolism, absorption rates, and interactions with other substances in the body can greatly affect how curcuminoids are processed, distributed, and eventually utilized. The study, although promising, does not delve into the intricacies of these processes in a human context, leaving a critical gap in our understanding. Furthermore, the potential side effects of curcuminoids in humans cannot be overlooked. While these compounds show therapeutic potential, they might also have adverse effects, particularly when consumed in specific quantities or in combination with other medications. Some individuals might be more susceptible to these side effects due to underlying health conditions or genetic factors, adding another layer of complexity to their clinical application. Addressing these challenges is

paramount before curcuminoids can be effectively and safely utilized in clinical settings.

Nature, particularly in the form of diverse plant and food sources, offers a rich unexplored pharmacopeia of extracts and compounds that may be applied to counteracting immune evasion and other disease pathologies. For example, numerous culinary spices have been acknowledged for their potential therapeutic attributes, for instance, cumin, turmeric, saffron, as well as green and black tea, and flax seeds are all enriched with curcuminoids that have applications to multiple health conditions (Thompson et al., 1996; Busquets et al., 2001; Abdullaev, 2002; Lai and Roy, 2004; Sharifi-Rad et al., 2020). This reaffirms the potential for natural extracts to serve as a promising wellspring for the discovery of innovative therapeutic agents, including those potentially capable of reversing immune escape. As such, these could offer new inroads into controlling the growth and metastasis of cancer. The continued exploration of these resources could unlock novel approaches in our collective fight against this disease, promoting not only a deeper understanding of the intricate mechanisms at play but also fostering the development of innovative modes of therapeutic interventions.

Methods

Synthesis of racemic curcuphenol and structural analogues

On 23 April 1990, specimens of the Halichondria sp., a massive orange sponge, were manually collected using SCUBA equipment at Solong-on, Siquijor Island, Philippines (09° 10′N, 123° 29′E). A voucher sample from this collection has been archived at the Netherlands Centre for Biodiversity Naturalis in Leiden, the Netherlands, under the voucher number RMNH POR. 5,872. To extract the active components, 15 g of lyophilized sponge material were treated with methanol (3 × 50 mL) at room temperature. Bioassay-guided fractionation of the crude methanol extract led to the identification of curcuphenol as the active compound. The constitution of curcuphenol obtained from the Halichondria sp. was unambiguously determined through analysis of the 1D and 2D nuclear magnetic resonance (NMR) as well as mass spectrometry (MS) data. However, its absolute configuration remains undetermined. (CANADIAN CANCER SOCIETY et al., 2007; Nohara et al., 2023). The synthesis of pure R or S curcuphenol in the laboratory is challenging. Therefore, we chose to undertake synthesis of a small library of curcuphenols analogues that either lack the chiral centre, PC-02-113 (**11**) or are racemic mixtures to see if we could find an analogue that had superior activity *in vivo*. The structures and the SwissADME Output for TSA and curcuphenol and PC-02-113 and PC-03-97-1 Analogues is shown in Supplementary Table S1.

Experimental procedures for the synthesis of racemic curcuphenol and analogues

The general synthetic scheme used to synthesize the curcuphenol analogs PC-03-97-1 (**7**), PC-03-97-2 (**8**), PC-03-93

(**9**), PC-03-99 (**10**), PC-02-113 (**11**) and racemic curcuphenol (**12**) is shown in Figure 6 Panel A. The specific reaction details for the synthesis of PC-03-97-1 (**7**) and PC-03-97-2 (**8**) starting from aldehyde **1** are given below. The exact same reaction conditions were used to make racemic curcuphenol (**12**) and the analogues **9, 10** and **11** from starting materials **13, 14, 15,** and **19**, respectively, so the specific details of those syntheses have not been repeated here.
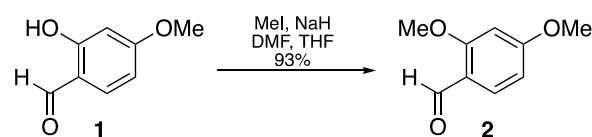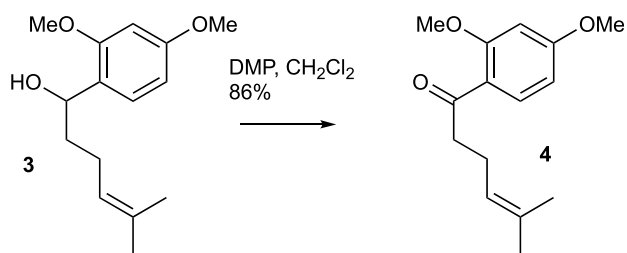

A suspension of NaH (172.6 mg, 60% in mineral oil, 4.32 mmol) in a DMF/THF mixture (5.4 mL, 4:1 v/v) was slowly combined with a solution containing 2-hydroxy-4-methoxybenzaldehyde (McGranahan and Swanton, 2017) (546.6 mg, 3.60 mmol) and MeI (0.46 mL, 7.32 mmol) in THF (3.6 mL) at 0°C. The cooling bath remained in place but was not replenished, and the mixture stirred for 18 h. The mixture was then diluted with Et$_2$O and washed with H$_2$O. The organic extract was dried over MgSO$_4$ and the solvent removed under vacuum. The resulting residue was purified through flash chromatography (silica gel, step gradient from 5: 100 EtOAc/hexanes to 15:100 EtOAc/hexanes), yielding compound 2 (552.5 mg, 93%) as a white solid. The ^{1}H NMR (400 MHz, CDCl3) showed δ 10.3 (s, 1H), 7.8 (d, J = 8.8 Hz, 1H), 6.5 (dd, J = 1.2, 8.4 Hz, 1H), 6.4 (d, J = 2.0 Hz, 1H), 3.9 (s, 3H), and 3.9 (s, 3H). The ^{13}C NMR (100 MHz, CDCl3) presented δ 188.5, 166.4, 163.8, 130.9, 119.2, 106.0, 98.1, 55.8, and 55.8.
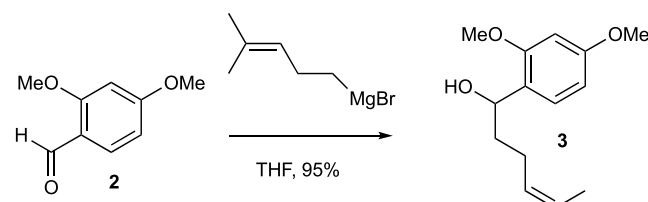

A mixture of Mg turnings (189.4 mg, 7.89 mmol) and a small amount of I2 in Et2O (1.0 mL) was combined with several drops of a 5-bromo-2-methyl-2-pentene (0.88 mL, 6.57 mmol) solution in Et2O (4.8 mL). After stirring for a few minutes, the yellow solution turned colorless, and the bromide solution was gradually added over an hour. The reaction mixture was then stirred under reflux for 1 h. A freshly prepared Grignard reagent was added to a solution of compound 2 (272.3 mg, 1.64 mmol) in THF (8 mL) at 0°C. The cooling bath was left in place but not recharged, and the mixture was stirred for 18 h. The reaction was quenched with saturated aqueous NH$_4$Cl solution and extracted with EtOAc three times. The combined organic extracts were washed with brine, dried over MgSO$_4$, and evaporated under vacuum. The residue was purified by flash chromatography (silica gel, step gradient from 5:100 EtOAc/hexanes to 15:100 EtOAc/hexanes) to yield compound 3 (389.6 mg, 95%) as a colorless oil. The 1H NMR (400 MHz, CDCl3) showed δ 7.19 (d, J = 8.4 Hz, 1H), 6.44–6.48 (m, 2H), 5.2 (tt, J = 1.2, 7.2 Hz, 1H), 4.8 (t, J = 6.4 Hz, 1H), 3.8 (s, 3H), 3.8 (s, 3H), 2.5 (bs, 1H), 1.98–2.16 (m, 2H), 1.72–1.88 (m, 2H), 1.7 (s, 3H), and 1.6 (s, 3H). The 13C NMR (100 MHz, CDCl3) displayed δ

160.2, 157.9, 132.0, 127.8, 125.3, 124.4, 104.2, 98.8, 70.5, 55.5, 55.4, 37.4, 25.9, 25.0, and 17.9. HRESIMS [M + Na]+ m/z 273.1462 (calculated for C15H22O3Na, 273.1467).

124.8, 104.1, 99.5, 75.0, 55.5, 42.3, 27.7, 25.8, 23.6, and 17.7. HRESIMS [M + Na]+ m/z 287.1619 (calculated for C16H24O3Na, 287.1623).

A solution of compound 3 (327.1 mg, 1.31 mmol) in CH$_2$Cl$_2$ (10 mL) was combined with DMP (714.9 mg, 1.64 mmol) at room temperature. After stirring for 30 min, TLC analysis confirmed the complete consumption of the starting material. Saturated aqueous NaHCO$_3$ solution was then added, and the mixture was extracted with CH$_2$Cl$_2$ three times. The combined organic extracts were washed with brine, dried over MgSO4, and evaporated under vacuum. The residue was purified using flash chromatography (silica gel, step gradient from 0:100 EtOAc/hexanes to 8:100 EtOAc/hexanes), yielding compound 4 (280.3 mg, 86%) as a colorless oil. The 1H NMR (400 MHz, CDCl3) showed δ 7.79 (d, J = 8.8 Hz, 1H), 6.5 (dd, J = 2.0, 8.8 Hz, 1H), 6.5 (d, J = 2.0 Hz, 1H), 5.2 (dt, J = 1.6, 7.2 Hz, 1H), 3.9 (s, 3H), 3.8 (s, 3H), 2.9 (t, J = 7.6 Hz, 2H), 2.3 (q, J = 7.6 Hz, 2H), 1.7 (s, 3H), and 1.6 (s, 3H). The 13C NMR (100 MHz, CDCl3) displayed δ 200.5, 164.4, 160.9, 132.9, 132.2, 123.9, 121.5, 105.2, 98.5, 55.7, 55.7, 43.9, 25.9, 23.5, and 17.8. HRESIMS [M + Na]+ m/z 271.1309 (calculated for C15H20O3Na, 271.1310).
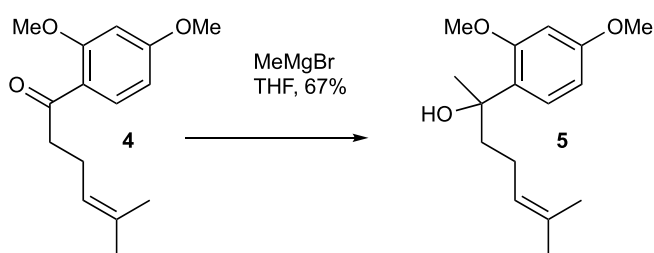
A solution of compound 4 (179.3 mg, 0.72 mmol) in THF (3 mL) had MeMgBr solution (0.32 mL, 3.0 M in Et$_2$O, 0.96 mmol) slowly added at 0°C. The mixture was stirred at room temperature for 2 h. The reaction mixture was then cooled to 0°C and quenched with saturated aqueous NH4Cl solution. The mixture was extracted with CH2Cl2 three times, and the combined organic extracts were washed with brine, dried over MgSO$_4$, and evaporated under vacuum. The residue was purified using flash chromatography (silica gel, step gradient from 0:100 EtOAc/hexanes to 7:100 EtOAc/hexanes), yielding compound 5 (128.1 mg, 67%) as a colorless oil. The ^{1}H NMR (400 MHz, CDCl3) showed δ 7.21 (d, J = 8.4 Hz, 1H), 6.5 (d, J = 2.4 Hz, 1H), 6.46 (dd, J = 2.4, 8.8 Hz, 1H), 5.1 (t, J = 6.8 Hz, 1H), 3.85 (s, 3H), 3.8 (bs, 3H), 3.8 (s, 3H), 1.79–2.01 (m, 4H), 1.65 (s, 3H), 1.54 (s, 3H), and 1.51 (s, 3H). The 13C NMR (100 MHz, CDCl3) displayed δ 159.8, 157.9, 131.6, 127.6, 127.5,

A solution of compound 5 (169.3 mg, 0.64 mmol) in CH2Cl2 (2 mL) had Et3SiH (0.13 mL, 0.81 mmol) added dropwise at −78°C. After stirring for 10 min, BF3. OEt2 (0.12 mL, 0.97 mmol) was added dropwise, and the mixture was stirred for an additional hour at −78°C. The mixture was then diluted with CH2Cl2 and washed with saturated aqueous NaHCO3 solution and water until neutral. The organic extract was dried over MgSO4 and evaporated under vacuum. The residue was purified using flash chromatography (silica gel, step gradient from 0:100 EtOAc/hexanes to 1:100 EtOAc/hexanes), yielding compound 6 (135.1 mg, 85%) as a colorless oil. The 1H NMR (400 MHz, CDCl3) showed δ 7.06 (d, J = 8.0 Hz, 1H), 6.45–6.48 (m, 2H), 5.10–5.15 (m, 1H), 3.802 (s, 3H), 3.8 (s, 3H), 3.1 (sixt, J = 7.2 Hz, 1H), 1.83–1.97 (m, 2H), and 1.47–1.68 (m, 8H). The 13C NMR (100 MHz, CDCl3) displayed δ 158.8, 158.2, 131.3, 128.6, 127.3, 125.1, 104.2, 98.7, 55.5, 55.5, 37.5, 31.5, 26.5, 25.9, 21.4, and 17.8. HRESIMS [M + H]+ m/z 249.1854 (calculated for C16H25O2, 249.1855).
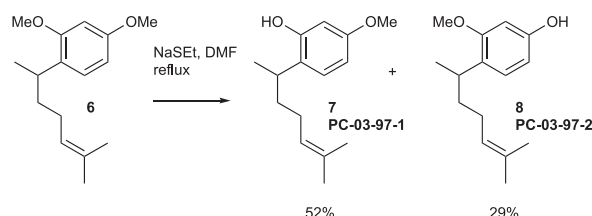
NaSEt (489.9 mg, 5.24 mmol) was mixed with DMF (2 mL) at 0°C, then warmed to room temperature. A solution of compound 6 (110.0 mg, 0.44 mmol) in DMF (1 mL) was added, and the mixture was stirred under reflux for 3 h. It was then cooled to 0°C, and 10% HCl (~3 mL) and CH2Cl2 (~15 mL) were added. The organic layer was washed twice with water, dried over MgSO4, and evaporated under vacuum. The residue was purified using flash chromatography (silica gel, step gradient from 0:100 EtOAc/hexanes to 10:100 EtOAc/hexanes), yielding compound 7 (PC-03-97-1) (54.2 mg, 52%) as a colorless oil and compound 8 (PC-03-97-2) (30.4 mg, 29%) as a light yellow oil.

For isomer 7: The ^{1}H NMR (600 MHz, CDCl3) showed δ 7.05 (d, J = 8.4 Hz, 1H), 6.5 (dd, J = 2.4, 8.4 Hz, 1H), 6.4 (d, J = 2.4 Hz, 1H), 5.14 (t, J = 7.2 Hz, 1H), 4.9 (bs, 1H), 3.8 (s, 3H), 2.9 (sixt, J = 7.2 Hz, 1H), 1.90–1.98 (m, 2H), 1.7 (s, 3H), 1.55–1.69 (m, 2H), 1.55 (s, 3H), and 1.23 (d, J = 7.2 Hz, 3H). The ^{13}C NMR (150 MHz, CDCl3) displayed δ 158.6, 154.1, 132.4, 127.7, 125.5, 124.8, 106.5, 101.9, 55.5, 37.6, 31.3, 26.2, 25.9, 21.4, and 17.9. HRESIMS [M - H]- m/z 233.1543 (calculated for C15H21O2, 233.1542).

For isomer 8: The ^{1}H NMR (600 MHz, CDCl3) showed δ 6.99 (d, J = 8.4 Hz, 1H), 6.4 (s, 1H), 6.4 (d, J = 7.8 Hz, 1H), 5.1 (t, J = 6.6 Hz, 1H), 4.8 (bs, 1H), 3.8 (s, 3H), 3.1 (sixt, J = 7.2 Hz, 1H), 1.82–1.96 (m, 2H), 1.47–1.69 (m, 8H), and 1.15 (d, J = 6.6 Hz, 3H). The ^{13}C NMR (150 MHz, CDCl3) displayed δ 158.

Tumour cell lines

TC-1 and A9 tumour cell lines were used to study immune evasion mechanisms and to investigate how tumours can escape immune surveillance (Smahel et al., 2003; Setiadi et al., 2005; Setiadi et al., 2007a; Setiadi et al., 2008). The TC-1 cell line is a mouse lung cancer cell line that originates from primary lung epithelial cells of a C57BL/6 mouse. To immortalize TC-1 cells, the LXSN16 amphitropic retrovirus vector was used, which contains Human Papillomavirus E6/E7 oncogenes. Additionally, the TC-1 cells were transformed with a pVEJB plasmid expressing the activated human H-Ras oncogene. These genetic modifications confer oncogenic properties to the cells, leading to their immortalization and tumour formation potential. The A9 cell line, on the other hand, is derived from the metastatic variant of TC-1 cells. This was achieved through *in vivo* immunization procedures in animals that carried the original TC-1 parental cells. The immunization promoted the selection of clones with improved immune resistance, resulting in the establishment of the A9 cell line, which exhibits characteristics of immune escape or immune editing. One notable difference between TC-1 and A9 cells is their MHC-I expression levels. While TC-1 cells display high MHC-I expression, A9 cells have nearly undetectable levels of MHC-I. To test the induction of MHC-I and TAP-1 expression in A9 cells after small molecule treatments, metastatic A9 cells were plated at a density of 3×10^5 onto a 6-well plate in 2 mL of DMEM. Twenty-four hours after plating, cells were subjected to one of the following treatments for 48 hours:1% dimethyl sulfoxide (Sigma) in DMEM (1% DMSO) as a vehicle control, 150 nmol of curcuphenol (provided by Dr. Raymond Anderson) or 40 ng of Recombinant Mouse Interferon-γ (IFNγ; R&D Systems) as a positive control. Curcuphenol stock was dissolved in DMSO. All compounds were diluted in 1% DMSO.

Evaluation of MHC-I surface expression by flow cytometry

Primary TC-1 tumour or metastatic A9 tumour cells, as shown in Figure 1, were plated in 6-well plates at a concentration of 1×10^3 cells per well in a 2 mL volume. Cells were treated with the indicated compound concentrations the following day and incubated for 48 h at 37°C. After incubation, cells were trypsinized, washed, and stained with APC-conjugated anti-mouse MHC-I (specifically anti-H-2K$_b$) antibody (cat. 141605; clone 25-D1.16; Biolegend) and analyzed by flow cytometry where viability was determined by aminoactinomycin (7AAD) viability stain (Biolegend). Primary TC-1 tumour cells served as a positive control for surface MHC-I expression, while vehicle alone (1% DMSO) was used as a negative control. Supplementary Table S2 displays the antibody panel used for FACS during the mouse tumour trial,

and Supplementary Table S3 lists the primer sequences used for RT-PCR.

Measuring the frequency of tumour infiltrating lymphocytes

For measuring the frequency if CD4 and CD8 populations within the tumour mass, tumour were resected and single cell suspensions were prepared and stained with APC-conjugated antibody against CD4 (553051, RM4-5, BD Bioscience) and PE-Cy7-conjugated antibody against CD8a (25-0081-82, 53-6.7, Affymetrix eBioscience) was used. The gating strategy has been described in our previous publication (Nohara et al., 2023; Saranchova et al., 2018).

Comparison of MHC-I cell surface induction by curcuphenol analogues

A9 cells were placed in 6-well plates with a density of 1×10^3 cells per well in a volume of 2 mL. On the subsequent day, the cells were exposed to specified concentrations of the compounds and incubated for 48 h at 37°C. Following the incubation period, the cells were treated with trypsin, washed, and then stained with APC-conjugated anti-mouse MHC-I (anti-H-2Kb, Biolegend). Flow cytometry analysis was conducted to evaluate the results.

For the sake of comparison, positive controls were implemented. Specifically, cells were subjected to treatment with either IFN-γ and or trichostatin A (TSA, Sigma-Aldrich) for 48h, which served to induce the expression of surface MHC-I. In contrast, a negative control was established using only the vehicle (1% DMSO). The experiments were repeated 2 times (n = 2) to accurately calculate the mean fluorescence MHC-I expression was calculated. Analogues with greater then 40% activity of TSA and with low cytotoxicity (cell viability within one standard deviation of 1% DMSO negative control) were selected as candidates for further analysis.

Induction by curcuphenols of T lymphocyte recognition of metastatic tumours

Carboxyfluorescein succinimidyl ester (CFSE) is a cell permeable fluorescent dye that covalently coupled to intracellular molecules and can therefore be retained within cells and dilute in fluorescent intensity as the cells divide. CFSE experiments were conducted using CD8$^+$ T lymphocytes from SIINFEKL-specific OT1 mice to determine if curcuphenol can induce antigen presentation of metastatic A9 Cells. Three groups were used to stimulated OT1 T lymphocytes recognition: A9 cells pulsed with SIINFEKL (Vehicle Control); A9 cells induced with IFNγ and pulsed with SIINFEKL (IFNγ); A9 cells induced with curcuphenol and pulsed with SIINFEKL (curcuphenol). The negative control consists of CD8$^+$ T lymphocytes from SIINFEKL-specific OT1 alone (negative CTRL). Evidently, IFNγ and curcuphenol-stimulated CD8$^+$ T lymphocytes from SIINFEKL-specific OT1 exhibited more proliferation than the controls. To compare T lymphocytes proliferation statistically among different treatment groups, the total T lymphocytes number from various treatment

groups at each generation was plotted and assessed using a one-way ANOVA with Tukey's multiple comparison test. p values less than 0.05 were deemed significant.

Determining the maximum tolerable dosages for curcuphenol synthetic analogues

Flow cytometry was employed to show that PC-02-113 and PC-03-97-1 curcuphenol analogues could trigger MHC-I expression on the cell surface 48 h post-treatment while maintaining minimal cytotoxicity. To identify the highest tolerable dose for curcuphenol analogues PC-02-113 and PC-03-97-1, various concentrations were assessed for toxicity. Dosages began at 1.0 mg/kg and increased to 3.5 mg/kg for both substances, reaching a final concentration of 5.2 mg/kg. The solubility of the compounds was the primary constraint in this experiment, as 1% DMSO is the maximum allowed concentration for intraperitoneal injections. Given these restrictions, 5.2 mg/kg was the largest intraperitoneal dosage employed. For each concentration of both compounds, three mice were examined, totaling nine mice per compound. Mice were observed for 14 days, and no indications of cytotoxicity were detected. Following the 14-day period, the mice underwent necropsy. No observable signs of toxicity or irregularities were found for either compound at any dosage. As a result, 5.2 mg/kg was selected as the dosage for subsequent studies.

Reverse transcription and real-time PCR

RNA was isolated using the Purelink™ RNA Mini Kit (Invitrogen, #12183-025), followed by DNase I (Ambion, #AM2222) treatment. RNA was then reverse transcribed into cDNA using the SuperScript® III First-Strand Synthesis System for RT-PCR (Invitrogen, #18080-051). Real-Time PCR (RT-PCR) was done using a 7,500 Fast Real-Time PCR system (Applied Biosystems) with the following parameters: 40 cycles (95°C denaturing 15 s, 60°C annealing for 1 min).

Maximum tolerated dose (MTD in mice)

All mouse experiments were approved by the Animal Care Committee at UBC. The highest tolerable doses for the selected compounds, PC-02-113 and PC-03-97-1, were evaluated *in vivo*. C57Bl/6 mice were given intraperitoneal (i.p.) injections of the compounds at three different concentrations: 1.0 mg/kg (n = 3), 3.5 mg/kg (n = 3), and 5.2 mg/kg (n = 3). Mice were monitored for 14 days for any clinical signs of toxicity, and a necropsy was performed at the end of the study. The highest MTD dose did not cause any adverse effects and was utilized for further experiments.

Pharmacokinetic study

To assess the pharmacokinetics (PK) of the curcuphenol analogues, a mass spectrometry assay was developed to measure the compounds in plasma. This assay was created by The Metabolomics Innovation Center

(TMIC) at UVic-Genome BC Proteomics Centre located in Victoria, British Columbia. Eight samples were sent to TMIC for PK design for identification of P02-113 and P03-97-1 in mouse plasma. To collect plasma, mice were anesthetized using isoflurane and blood was collected by cardiac puncture. Plasma was isolated from blood in a potassium-EDTA coated Tube with K2E (BD Microtainer) and centrifugation at 10,000 x g for 1 min. Plasma was transferred to a cryovial and stored at −20°C before being shipped on dry ice. TMIC used a chemical derivatization—UPLC-MMR/MS method to create a quantitative analysis tool for the compounds using dansyl chloride (DAN.CI) as the derivatizing reagent. 13C- labeled DAN. CI was used to produce stable isotope-labeled internal standards (ISs). All tests were performed using an UPLC-4000 QTRAP system with ESI and (+) ion detection using C18 column and acetonitrile-water-formic acid as the mobile phase.

For the PK analysis of P02-113 and P03-97-1, mice were injected i. p. and anesthetized before blood was collected by cardiac puncture at five time points (5 min, 10 min, 30 min, 1h and 6 h). Time points were chosen based on the published data for TSA (0.5 mg/kg), a drug of similar chemical structure and size to the compounds. Three female C57BL/6 mice, between the ages 6–8 weeks, were used for each compound for each time point, giving a total 12 mice per compound. All mice were injected at the highest maximum tolerated dose (5.2 mg/kg) and plasma was prepared and stored as previously described above.

Treatment of tumour-bearing mice with identified compounds

4×10^5 metastatic A9 cells suspended in HBSS were subcutaneously (s.c.) transplanted into the right flank of 32 eight-week-old female C57Bl/6 mice. Starting 7 days after tumour injection, mice in each tumour group were treated daily by i. p. injection with either one of the identified compounds (n = 8 for each compound), TSA positive control (n = 8), or vehicle alone (n = 8) for 2 weeks. Body weight and tumours were measured every 2–4 days, with more frequent measurements as tumour size increased. Tumour volume was calculated as follows: tumour volume = length x width^2. Tumour growth rate assessment methods were based on previously described techniques (Setiadi et al., 2008).

Survival for mice with A9 tumours was determined based on the overall weight of the mouse and tumour volume. Mice were euthanized if they lost 15–20% of their initial weight or tumours grew larger than 1 cm³, in accordance with animal ethics guidelines.

Statistical analysis

Data were examined using RStudio and Excel. An ANOVA test was utilized to establish statistical significance between controlled test groups, with a p-value of ≤0.05 deemed significant.

Data availability statement

The original contributions presented in the study are included in the article/Supplementary Materials, further inquiries can be directed to the corresponding author.

Ethics statement

The animal study was approved by Animal Care Committee at the University of British Columbia. The study was conducted in accordance with the local legislation and institutional requirements.

Author contributions

SE: Data curation, Formal Analysis, Investigation, Methodology, Writing–original draft, Writing–revision and editing. LN: Data curation, Formal Analysis, Investigation, Methodology, Writing–original draft, Writing–revision and editing. SD: Investigation, Methodology, Writing–original draft. IS: Investigation, Methodology, Validation, Writing–original draft. LM: Formal Analysis, Investigation, Methodology, Writing–original draft. KC: Formal Analysis, Validation, Writing–revision and editing. EG: Data curation, Formal Analysis, Methodology, Validation, Writing–revision and editing. CP: Formal Analysis, Investigation, Methodology, Validation, Writing–revision and editing. DW: Data curation, Formal Analysis, Investigation, Methodology, Validation, Writing–revision and editing. PC: Formal Analysis, Investigation, Validation, Writing–original draft. RA: Conceptualization, Writing–original draft, Writing–revision and editing. WJ: Conceptualization, Supervision, Visualization, Writing–original draft, Writing–revision and editing.

Funding

Acknowledgments

Conflict of interest

WJ is a founder and SE, LN, SD, IS, KC, CP, PC, RA and WJ are shareholders in CaVa Healthcare Inc, the holder of UBC licenses and patents related to this work.

The remaining authors declare that the research was conducted in the absence of any commercial or financial relationships that could be construed as a potential conflict of interest.

Publisher's note

All claims expressed in this article are solely those of the authors and do not necessarily represent those of their affiliated organizations, or those of the publisher, the editors and the reviewers. Any product that may be evaluated in this article, or claim that may be made by its manufacturer, is not guaranteed or endorsed by the publisher.

Supplementary material

The Supplementary Material for this article can be found online at: https://www.frontiersin.org/articles/10.3389/fntpr.2023.1281061/full#supplementary-material

References

Abdullaev, F. I. (2002). Cancer chemopreventive and tumoricidal properties of saffron (Crocus sativus L.). *Exp. Biol. Med. (Maywood)* 227 (1), 20–25. doi:10.1177/153537020222700104

Alimonti, J., Zhang, Q. J., Gabathuler, R., Reid, G., Chen, S. S., and Jefferies, W. A. (2000). TAP expression provides a general method for improving the recognition of malignant cells *in vivo*. *Nat. Biotechnol.* 18 (5), 515–520. doi:10.1038/75373

Alpan, R. S., Zhang, M., and Pardee, A. B. (1996). Cell cycle-dependent expression of TAP1, TAP2, and HLA-B27 messenger RNAs in a human breast cancer cell line. *Cancer Res.* 56 (19), 4358–4361.

Andratschke, M., Pauli, C., Stein, M., Chaubal, S., and Wollenberg, B. (2003). MHC-class I antigen expression on micrometastases in bone marrow of patients with head and neck squamous cell cancer. *Anticancer Res.* 23 (2B), 1467–1471.

Behery, F. A., Sallam, A. A., and El Sayed, K. A. (2012). Mannich- and Lederer-Manasse-based analogues of the natural product S-(+)-curcuphenol as cancer proliferation and migration inhibitors. *Medchemcomm* 3 (10), 1309–1315. doi:10.1039/c2md20185b

Blades, R. A., Keating, P. J., McWilliam, L. J., George, N. J., and Stern, P. L. (1995). Loss of HLA class I expression in prostate cancer: implications for immunotherapy. *Urology* 46 (5), 681–687. doi:10.1016/s0090-4295(99)80301-x

Busquets, S., Carbo, N., Almendro, V., Quiles, M. T., Lopez-Soriano, F. J., and Argiles, J. M. (2001). Curcumin, a natural product present in turmeric, decreases tumor growth but does not behave as an anticachectic compound in a rat model. *Cancer Lett.* 167 (1), 33–38. doi:10.1016/s0304-3835(01)00456-6

Cabrera, C. M., Lopez-Nevot, M. A., Jimenez, P., and Garrido, F. (2005). Involvement of the chaperone tapasin in HLA-B44 allelic losses in colorectal tumors. *Int. J. Cancer* 113 (4), 611–618. doi:10.1002/ijc.20526

CANADIAN CANCER SOCIETY; NATIONAL CANCER INSTITUTE OF CANADA; STATISTICS CANADA P; TERRITORIAL CANCER REGISTRIES; CANADA PHAO; Canadian Cancer Statistics. 2007.

Carbone, F. R., Sterry, S. J., Butler, J., Rodda, S., and Moore, M. W. (1992). T cell receptor alpha-chain pairing determines the specificity of residue 262 within the Kb-restricted, ovalbumin257-264 determinant. *Int. Immunol.* 4 (8), 861–867. doi:10.1093/intimm/4.8.861

Chang, C. C., Ogino, T., Mullins, D. W., Oliver, J. L., Yamshchikov, G. V., Bandoh, N., et al. (2006). Defective human leukocyte antigen class I-associated antigen presentation caused by a novel β2-microglobulin loss-of-function in melanoma cells. *J. Biol. Chem.* 281 (27), 18763–18773. doi:10.1074/jbc.m511525200

Cichewicz, R. H., Clifford, L. J., Lassen, P. R., Cao, X. L., Freedman, T. B., Nafie, L. A., et al. (2005). Stereochemical determination and bioactivity assessment of (S)-(+)-curcuphenol dimers isolated from the marine sponge Didiscus aceratus and synthesized through laccase biocatalysis. *Bioorgan Med. Chem.* 13 (19), 5600–5612. doi:10.1016/j.bmc.2005.06.020

Cragg, G. M. L., Kingston, D. G. I., and Newman, D. J. (2012). *Anticancer agents from natural products*. 2nd ed. Boca Raton: CRC Press; xv, 751.

Dada, S., Ellis, S. L. S., Wood, C., Nohara, L. L., Dreier, C., Garcia, N. H., et al. (2022). Specific cannabinoids revive adaptive immunity by reversing immune evasion mechanisms in metastatic tumours. *Front. Immunol.* 13, 982082. doi:10.3389/fimmu.2022.982082

Dada, S., Ellis, S. L., Wood, C., Nohara, L. L., Dreier, C., Garcia, N. H., et al. (2023). Specific cannabinoids revive adaptive immunity by reversing immune evasion mechanisms in metastatic tumours. *Front. Immunol.* 13, 982082. doi:10.3389/fimmu.2022.982082

Dhatchinamoorthy, K., Colbert, J. D., and Rock, K. L. (2021). Cancer immune evasion through loss of MHC class I antigen presentation. *Front. Immunol.* 12, 636568. doi:10.3389/fimmu.2021.636568

Diedrich, G., Bangia, N., Pan, M., and Cresswell, P. (2001). A role for calnexin in the assembly of the MHC class I loading complex in the endoplasmic reticulum. *J. Immunol.* 166 (3), 1703–1709. doi:10.4049/jimmunol.166.3.1703

Ellis, S. L. S., Dada, S., Nohara, L. L., Saranchova, I., Munro, L., Pfeifer, C. G., et al. (2023). Curcuphenol possesses an unusual histone deacetylase enhancing activity that counters immune escape in metastatic tumours. *Front. Pharmacol.* 14, 1119620. doi:10.3389/fphar.2023.1119620

El Sayed, K. A., Yousaf, M., Hamann, M. T., Avery, M. A., Kelly, M., and Wipf, P. (2002). Microbial and chemical transformation studies of the bioactive marine sesquiterpenes (S)-(+)-curcuphenol and -curcudiol isolated from a deep reef collection of the Jamaican sponge Didiscus oxeata. *J. Nat. Prod.* 65 (11), 1547–1553. doi:10.1021/np020213x

Falk, K., Rötzschke, O., Stevanović, S., Jung, G., and Rammensee, H. G. (1991). Allele-specific motifs revealed by sequencing of self-peptides eluted from MHC molecules. *Nature* 351 (6324), 290–296. doi:10.1038/351290a0

Fridman, W. H. (2018). From cancer immune surveillance to cancer immunoediting: birth of modern immuno-oncology. *J. Immunol.* 201 (3), 825–826. doi:10.4049/jimmunol.1800827

Fusetani, N., Sugano, M., Matsunaga, S., and Hashimoto, K. (1987). (+)-Curcuphenol and dehydrocurcuphenol, novel sesquiterpenes which inhibit H,K-atpase, from a marine sponge epipolasis sp. *Experientia* 43 (11-12), 1234–1235. doi:10.1007/bf01945540

Gabathuler, R., Reid, G., Kolaitis, G., Driscoll, J., and Jefferies, W. A. (1994). Comparison of cell lines deficient in antigen presentation reveals a functional role for TAP-1 alone in antigen processing. *J. Exp. Med.* 180 (4), 1415–1425. doi:10.1084/jem.180.4.1415

Gabathuler, R., Alimonti, J., Zhang, Q. J., Kolaitis, G., Reid, G., and Jefferies, W. A. (1998). Surrogate antigen processing mediated by TAP-dependent antigenic peptide secretion. *J. Cell Biol.* 140 (1), 17–27. doi:10.1083/jcb.140.1.17

Gaspar, H., Feio, S. S., Rodrigues, A. I., and Van Soest, R. (2004). Antifungal activity of (+)-Curcuphenol, a metabolite from the marine sponge didiscus oxeata. *Mar. Drugs* 2 (1), 8–13. doi:10.3390/md201008

Gaspar, H., Moiteiro, C., Sardinha, J., and Gonzalez-Coloma, A. (2008). Bioactive semisynthetic derivatives of (S)-(+)-curcuphenol. *Nat. Prod. Commun.* 3 (9), 1934578X0800300–64. doi:10.1177/1934578x0800300911

Hogquist, K. A., Jameson, S. C., Heath, W. R., Howard, J. L., Bevan, M. J., and Carbone, F. R. (1994). T cell receptor antagonist peptides induce positive selection. *Cell* 76 (1), 17–27. doi:10.1016/0092-8674(94)90169-4

Huang, M., Lu, J.-J., and Ding, J. (2021). Natural products in cancer therapy: past, present and future. *Nat. Prod. Bioprospecting* 11 (1), 5–13. doi:10.1007/s13659-020-00293-7

Jefferies, W. A., Kolaitis, G., and Gabathuler, R. (1993). IFN-gamma-induced recognition of the antigen-processing variant CMT. 64 by cytolytic T cells can be replaced by sequential addition of beta 2 microglobulin and antigenic peptides. *J. Immunol. (Baltim. Md. 1950).* 151 (6), 2974–2985.

Kamarashev, J., Ferrone, S., Seifert, B., Boni, R., Nestle, F. O., Burg, G., et al. (2001). TAP1 down-regulation in primary melanoma lesions: an independent marker of poor prognosis. *Int. J. Cancer* 95 (1), 23–28. doi:10.1002/1097-0215(20010120)95:1<23::aid-ijc1004>3.0.co;2-4

Kitamura, K., Matsuda, A., Motoya, S., and Takeda, A. (1997). CD45-associated protein is a lymphocyte-specific membrane protein expressed in two distinct forms. *Eur. J. Immunol.* 27 (2), 383–388. doi:10.1002/eji.1830270207

Lai, P. K., and Roy, J. (2004). Antimicrobial and chemopreventive properties of herbs and spices. *Curr. Med. Chem.* 11 (11), 1451–1460. doi:10.2174/0929867043365107

Lankat-Buttgereit, B., and Tampé, R. (2002). The transporter associated with antigen processing: function and implications in human diseases. *Physiol. Rev.* 82 (1), 187–204. doi:10.1152/physrev.00025.2001

Lou, Y., Basha, G., Seipp, R. P., Cai, B., Chen, S. S., Moise, A. R., et al. (2008). Combining the antigen processing components TAP and Tapasin elicits enhanced tumor-free survival. *Clin. cancer Res.* 14 (5), 1494–1501. doi:10.1158/1078-0432.ccr-07-1066

Lou, Y., Seipp, R. P., Cai, B., Chen, S. S., Vitalis, T. Z., Choi, K. B., et al. (2007). Tumour immunity and T cell memory are induced by low dose inoculation with a non-replicating adenovirus encoding TAP1. *Vaccine* 25 (12), 2331–2339. doi:10.1016/j.vaccine.2006.11.064

Marusina, K., Reid, G., Gabathuler, R., Jefferies, W., and Monaco, J. J. (1997). Novel peptide-binding proteins and peptide transport in normal and TAP-deficient microsomes. *Biochemistry* 36 (4), 856–863. doi:10.1021/bi9619738

McDermott, R. S., Beuvon, F., Pauly, M., Pallud, C., Vincent-Salomon, A., Mosseri, V., et al. (2002). Tumor antigens and antigen-presenting capacity in breast cancer. *Pathobiology* 70 (6), 324–332. doi:10.1159/000071272

McGranahan, N., and Swanton, C. (2017). Clonal heterogeneity and tumor evolution: past, present, and the future. *Cell* 168 (4), 613–628. doi:10.1016/j.cell.2017.01.018

Mehta, A. M., Jordanova, E. S., Kenter, G. G., Ferrone, S., and Fleuren, G. J. (2008). Association of antigen processing machinery and HLA class I defects with clinicopathological outcome in cervical carcinoma. *Cancer Immunol. Immunother.* 57 (2), 197–206. doi:10.1007/s00262-007-0362-8

Naoe, M., Marumoto, Y., Ishizaki, R., Ogawa, Y., Nakagami, Y., and Yoshida, H. (2002). Correlation between major histocompatibility complex class I molecules and CD8+ T lymphocytes in prostate, and quantification of CD8 and interferon-gamma mRNA in prostate tissue specimens. *BJU Int.* 90 (7), 748–753. doi:10.1046/j.1464-410x.2002.02993.x

Newman, D. J., and Cragg, G. M. (2016). Natural products as sources of new drugs from 1981 to 2014. *J. Nat. Prod.* 79 (3), 629–661. doi:10.1021/acs.jnatprod.5b01055

Nohara, L. L., Ellis, S. L. S., Dreier, C., Dada, S., Saranchova, I., Choi, K. B., et al. (2023). A novel cell-based screen identifies chemical entities that reverse the immune-escape phenotype of metastatic tumours. *Front. Pharmacol.* 14, 1119607. doi:10.3389/fphar.2023.1119607

Pishesha, N., Harmand, T. J., and Ploegh, H. L. (2022). A guide to antigen processing and presentation. *Nat. Rev. Immunol.* 22 (12), 751–764. doi:10.1038/s41577-022-00707-2

Rodrigo, G., Almanza, G. R., Cheng, Y., Peng, J., Hamann, M., Duan, R. D., et al. (2010). Antiproliferative effects of curcuphenol, a sesquiterpene phenol. *Fitoterapia* 81 (7), 762–766. doi:10.1016/j.fitote.2010.04.001

Sakkal, S., Miller, S., Apostolopoulos, V., and Nurgali, K. (2016). Eosinophils in cancer: favourable or unfavourable? *Curr. Med. Chem.* 23 (7), 650–666. doi:10.2174/0929867323666160119094313

Saranchova, I., Han, J., Huang, H., Fenninger, F., Choi, K. B., Munro, L., et al. (2016). Discovery of a metastatic immune escape mechanism initiated by the loss of expression of the tumour biomarker interleukin-33. *Sci. Rep-Uk* 6 (1), 30555. doi:10.1038/srep30555

Saranchova, I., Han, J., Zaman, R., Arora, H., Huang, H., Fenninger, F., et al. (2018). Type 2 innate lymphocytes actuate immunity against tumours and limit cancer metastasis. *Sci. Rep.* 8 (1), 2924. doi:10.1038/s41598-018-20608-6

Seliger, B. (2016). Molecular mechanisms of HLA class I-mediated immune evasion of human tumors and their role in resistance to immunotherapies. *HLA* 88 (5), 213–220. doi:10.1111/tan.12898

Setiadi, A. F., David, M. D., Chen, S. S., Hiscott, J., and Jefferies, W. A. (2005). Identification of mechanisms underlying transporter associated with antigen processing deficiency in metastatic murine carcinomas. *Cancer Res.* 65 (16), 7485–7492. doi:10.1158/0008-5472.can-03-3734

Setiadi, A. F., David, M. D., Seipp, R. P., Hartikainen, J. A., Gopaul, R., and Jefferies, W. A. (2007a). Epigenetic control of the immune escape mechanisms in malignant carcinomas. *Mol. Cell Biol.* 27 (22), 7886–7894. doi:10.1128/mcb.01547-07

Setiadi, A. F., David, M. D., Seipp, R. P., Hartikainen, J. A., Gopaul, R., and Jefferies, W. A. (2007b). Epigenetic control of the immune escape mechanisms in malignant carcinomas. *Mol. Cell. Biol.* 27 (22), 7886–7894. doi:10.1128/mcb.01547-07

Setiadi, A. F., Omilusik, K., David, M. D., Seipp, R. P., Hartikainen, J., Gopaul, R., et al. (2008). Epigenetic enhancement of antigen processing and presentation promotes immune recognition of tumors. *Cancer Res.* 68 (23), 9601–9607. doi:10.1158/0008-5472.can-07-5270

Shankaran, V., Ikeda, H., Bruce, A. T., White, J. M., Swanson, P. E., Old, L. J., et al. (2001). IFNγ and lymphocytes prevent primary tumour development and shape tumour immunogenicity. *Nature* 410 (6832), 1107–1111. doi:10.1038/35074122

Sharifi-Rad, J., Rayess, Y. E., Rizk, A. A., Sadaka, C., Zgheib, R., Zam, W., et al. (2020). Turmeric and its major compound curcumin on health: bioactive effects and safety profiles for food, pharmaceutical, biotechnological and medicinal applications. *Front. Pharmacol.* 11, 01021. doi:10.3389/fphar.2020.01021

Smahel, M., Síma, P., Ludvíková, V., Marinov, I., Pokorná, D., and Vonka, V. (2003). Immunisation with modified HPV16 E7 genes against mouse oncogenic TC-1 cell sublines with downregulated expression of MHC class I molecules. *Vaccine* 21 (11-12), 1125–1136. doi:10.1016/s0264-410x(02)00519-4

Soflaei, S. S., Momtazi-Borojeni, A. A., Majeed, M., Derosa, G., Maffioli, P., and Sahebkar, A. (2018). Curcumin: a natural pan-HDAC inhibitor in cancer. *Curr. Pharm. Des.* 24 (2), 123–129. doi:10.2174/1381612823666171114165051

Spies, T., Cerundolo, V., Colonna, M., Cresswell, P., Townsend, A., and DeMars, R. (1992). Presentation of viral antigen by MHC class I molecules is dependent on a putative peptide transporter heterodimer. *Nature* 355 (6361), 644–646. doi:10.1038/355644a0

Stutman, O. (1974). Tumor development after 3-methylcholanthrene in immunologically deficient athymic-nude mice. *Science* 183 (4124), 534–536. doi:10.1126/science.183.4124.534

Thompson, L. U., Rickard, S. E., Orcheson, L. J., and Seidl, M. M. (1996). SHORT COMMUNICATION: flaxseed and its lignan and oil components reduce mammary tumor growth at a late stage of carcinogenesis. *Carcinogenesis* 17 (6), 1373–1376. doi:10.1093/carcin/17.6.1373

Vitalis, T. Z., Zhang, Q. J., Alimonti, J., Chen, S. S., Basha, G., Moise, A., et al. (2005). Using the TAP component of the antigen-processing machinery as a molecular adjuvant. *PLoS Pathog.* 1 (4), e36. doi:10.1371/journal.ppat.0010036

Wright, A. E., Pomponi, S. A., Mcconnell, O. J., Kohmoto, S., and Mccarthy, P. J. (1987). (+)-Curcuphenol and (+)-Curcudiol, sesquiterpene phenols from shallow and deep-water collections of the marine sponge didiscus-flavus. *J. Nat. Prod.* 50 (5), 976–978. doi:10.1021/np50053a042

Zhang, H., Melamed, J., Wei, P., Cox, K., Frankel, W., Bahnson, R. R., et al. (2003). Concordant down-regulation of proto-oncogene PML and major histocompatibility antigen HLA class I expression in high-grade prostate cancer. *Cancer Immun.* 3, 2.

Zhang, Q. J., Alimonti, J., Chen, S. S., Moise, A., Tiong, J., and Jefferies, W. A. (2002). "Over-expression of TAP's augments immune responses in normal mice," in *FASEB JOURNAL (Vol. 16, No. 4, pp. A312-A312)* (9650 ROCKVILLE PIKE, BETHESDA, MD 20814-3998 USA: FEDERATION AMER SOC EXP BIOL).

Zhang, Q. J., Seipp, R. P., Chen, S. S., Vitalis, T. Z., Li, X. L., Choi, K. B., et al. (2007). TAP expression reduces IL-10 expressing tumor infiltrating lymphocytes and restores immunosurveillance against melanoma. *Int. J. cancer* 120 (9), 1935–1941. doi:10.1002/ijc.22371

Zheng, B., and McClements, D. J. (2020). Formulation of more efficacious curcumin delivery systems using colloid science: enhanced solubility, stability, and bioavailability. *Molecules* 25 (12), 2791. doi:10.3390/molecules25122791